

Coherent and controllable enhancement of light-harvesting efficiency

Stefano Tomasi,¹ Sima Baghbanzadeh,^{2,3} Saleh Rahimi-Keshari,^{2,3,4} and Ivan Kassal^{1,*}

¹*School of Chemistry and University of Sydney Nano Institute, University of Sydney NSW 2006, Australia*

²*School of Physics, Institute for Research in Fundamental Sciences (IPM), P.O. Box 19395-5531, Tehran, Iran*

³*Center for Quantum Information and Control, University of New Mexico, Albuquerque NM 87131, USA*

⁴*Institut für Theoretische Physik, Leibniz Universität Hannover, 30167 Hannover, Germany*

Spectroscopic experiments on photosynthetic complexes have identified long-lived coherences, suggesting that coherent effects can be relevant in disordered and noisy light-harvesting systems. However, there is limited experimental evidence that light-harvesting processes can be more efficient due to a coherent effect, largely due to the difficulty of turning coherences on and off to create an experimental control. Here, we show that coherence can be used to enhance light harvesting, starting from a model system with controllable initial states. Specifically, we consider a three-site system, comprising two identical coupled donors, one of which is coupled to an acceptor. Coupling within the donor dimer results in two delocalised eigenstates that can be addressed using different light modes, allowing a coherent light source to enhance exciton populations on either donor by controlling only the phase between two exciting modes. Coherently controlling the excitation in this way can significantly enhance the light-harvesting efficiency relative to incoherent excitation. Our proposal would allow for the first unambiguous demonstration of light harvesting enhanced by intermolecular coherence, as well as demonstrate the potential for coherent control of excitonic energy transfer.

Observations of long-lasting coherences in photosynthetic pigment-protein complexes [1–5], previously thought to be too strongly coupled to their environment to support coherent effects, have raised the question of whether coherence can play a role in molecular light-harvesting processes [1, 6–11]. The question remains open, despite arguments that the observed coherences are dominantly vibrational or vibronic [12–14] and that, in either event, they could not be induced by incoherent sunlight [8, 15–17]. Nevertheless, theoretical studies have proposed that, even in those circumstances, there are mechanisms by which coherences could enable significant enhancements of light-harvesting efficiencies [8, 18–25]. In most of those works, as in this one, efficiency is defined as the probability of an excitation being successfully transferred to a target acceptor, which, in many cases, eventually leads to charge transfer or another means of harvesting the excitation energy. Aside from providing insight into the relevance of quantum effects in biological systems, research on this topic is also motivated by the potential application of these concepts to the design of novel artificial light-harvesting devices [6, 11].

Direct experimental evidence of an efficiency enhancement due to intermolecular coherence is lacking for two reasons. First, experiments so far have focused on observing coherences in isolated systems, with no acceptor for the excitations to be transferred to, making them unable to relate coherence to efficiency. Second, to ensure that a particular enhancement is due to coherence and not a confounding factor, it would be necessary to be able to switch coherence on and off without affecting other experimental variables. This kind of control is often not possible in existing light harvesting systems; for example, altering their molecular structures often causes significant changes to their overall energy landscape [24].

The only demonstrations of coherent enhancements have been experiments showing that the efficiency of excitation transfer from one molecule can be increased through adaptive coherent control [26, 27]. These experiments targeted intramolecular (often vibrational [27]) coherences within the donor, leaving the effect of intermolecular coherences on efficiency unobserved. The-

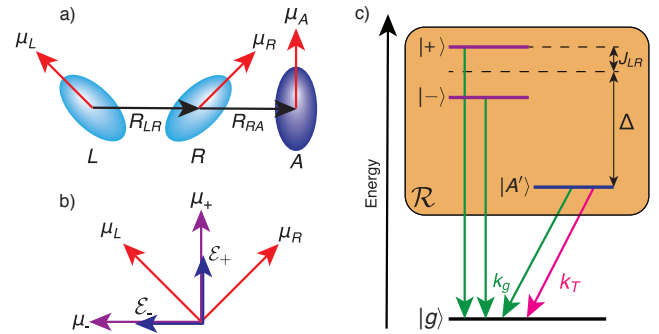


Figure 1. The light-harvesting system under investigation. **(a)** Two identical donor sites (L and R) are coupled to each other and to an acceptor (A). Also shown are the transition dipole moments μ of the sites, which lie in the plane of the paper. **(b)** The transition dipole moments of L and R are compared to those of the eigenstates $|+\rangle$ and $|-\rangle$. The light is coming into the page, with light component \mathcal{E}_{\pm} assumed parallel to μ_{\pm} . **(c)** The eigenstates of the model and the dissipation pathways. The dissipation within the excited-state manifold (orange) is described by a non-secular Redfield tensor \mathcal{R} , meaning it cannot be represented using simple rate processes. The acceptor's excited state is lower in energy compared to the donors to make the donor-to-acceptor excitation transfer energetically favourable.

oretical work has shown that multi-chromophoric light harvesting could also be controlled [28, 29], but the final pulse sequences produced by sophisticated optimisation algorithms can be difficult to understand intuitively.

Here, we address the problem from the bottom up. Instead of describing existing light-harvesting systems, our goal is to design a minimally complex light-harvesting system whose efficiency can be directly monitored and whose coherence can be externally controlled. The ability to compare light-harvesting efficiencies in the presence and absence of coherence would permit the first definitive demonstration of light-harvesting enhanced by intermolecular coherence.

Our model system consisting of two identical donor sites (e.g., molecules) and an acceptor site (Figure 1a).

The acceptor's excited state is significantly red shifted compared to the donors', ensuring that the donor-to-acceptor excitation transfer is both irreversible and spectrally resolvable. Excitonic coupling between the donors forms two eigenstates that are delocalised across the donor dimer and that can be addressed by different light modes. Using optical phase control—i.e., changing only the phases but not the intensity of the light—the system can be prepared in a wide range of coherent and incoherent initial states [23, 29–31]. By measuring the proportion of excitations successfully transferred to the acceptor (as opposed to lost to recombination), we can compare energy-transfer efficiencies for different initial states and unambiguously demonstrate the influence of excitonic coherence on light-harvesting efficiency. In particular, certain superpositions represent excitations that are mostly localised on particular sites, allowing for efficiency enhancements if excitations are localised close to the acceptor (Figure 2).

We treat the system with a Frenkel-type (tight-binding) Hamiltonian

$$H_S = \sum_u \epsilon_u |u\rangle\langle u| + \sum_{u \neq v} J_{uv} |u\rangle\langle v|, \quad (1)$$

where $|u\rangle$ represents an excitation localised on site u with energy ϵ_u and J_{uv} is the coupling between sites u and v . We assume dipole-dipole intersite couplings

$$J_{uv} = \frac{1}{4\pi\epsilon R_{uv}^3} \left[\boldsymbol{\mu}_{ug} \cdot \boldsymbol{\mu}_{vg} - 3 \left(\boldsymbol{\mu}_{ug} \cdot \hat{\mathbf{R}}_{uv} \right) \left(\boldsymbol{\mu}_{vg} \cdot \hat{\mathbf{R}}_{uv} \right) \right], \quad (2)$$

where ϵ is the dielectric constant, $\boldsymbol{\mu}_{ug}$ is the ground-to-excited-state transition dipole moment of site u , \mathbf{R}_{uv} is the distance between two sites, $R_{uv} \equiv |\mathbf{R}_{uv}|$ and $\hat{\mathbf{R}}_{uv} = \mathbf{R}_{uv}/R_{uv}$. We denote the eigenstates of H_S as $|a\rangle$, with energies E_a , shown in Figure 1c.

Coupling the system to a bath gives a total Hamiltonian

$$H = H_S + H_{SB} + H_B, \quad (3)$$

where the bath consists of an independent set of harmonic oscillators on each site,

$$H_B = \hbar \sum_{u,\xi} \omega_\xi b_\xi^{(u)\dagger} b_\xi^{(u)} \quad (4)$$

where $b_\xi^{(u)\dagger}$ and $b_\xi^{(u)}$ are the creation and annihilation operators for mode ξ on site u . The system-bath coupling is assumed to be linear,

$$H_{SB} = \hbar \sum_{u,\xi} \omega_\xi g_\xi |u\rangle\langle u| \left(b_\xi^{(u)\dagger} + b_\xi^{(u)} \right). \quad (5)$$

The time evolution of the system's reduced density operator (RDO) ρ is given by the master equation

$$\dot{\rho} = -\frac{i}{\hbar} [H_S, \rho] + \mathcal{D}\rho, \quad (6)$$

where the dissipator \mathcal{D} encodes the non-unitary evolution. We divide \mathcal{D} into three superoperators (illustrated in Figure 1c),

$$\mathcal{D} = \mathcal{R} + \mathcal{L}_g + \mathcal{L}_T, \quad (7)$$

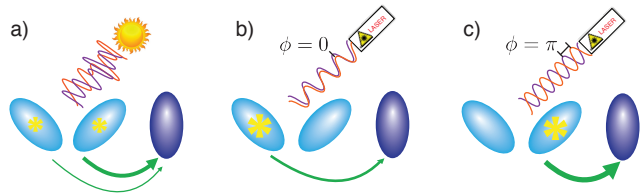


Figure 2. Mechanism of coherent efficiency enhancement. (a) Incoherent light excites a mixture of donor eigenstates, while coherent light (b–c) can be used to address the individual $|+\rangle$ and $|-\rangle$ eigenstates and localise excitations to either donor site. The localisation is achieved by controlling only the relative phase between the two light modes and not the spectrum of the light. The donor-acceptor transfer rate—and therefore the light-harvesting efficiency—can be significantly enhanced or diminished compared to the incoherent case if excitations are localised on R or L respectively.

where \mathcal{R} describes the effect of H_{SB} on the system—and therefore the evolution of excited states due to interactions with the thermal bath—and where the additional terms \mathcal{L}_g and \mathcal{L}_T describe the relaxation of the excited states to a ground state $|g\rangle$ through processes that are not accounted for in the Hamiltonian H .

Excitons have a finite lifetime due to radiative and non-radiative recombination, which, if we assume an equal decay rate k_g from each excited state, is described by the superoperator

$$\mathcal{L}_g \rho = k_g \sum_a \left(|g\rangle\langle a| \rho |a\rangle\langle g| - \frac{1}{2} \left\{ |a\rangle\langle a|, \rho \right\} \right), \quad (8)$$

where $\{\cdot, \cdot\}$ denotes an anticommutator.

We also define a *target* process that causes a decay to $|g\rangle$ exclusively from a particular eigenstate $|T\rangle$ at rate k_T . This process can, for example, represent a successful separation of an exciton into charge carriers, or simply an external observation of a donor-acceptor transfer event. We model the target process as

$$\mathcal{L}_T \rho = k_T \left(|g\rangle\langle T| \rho |T\rangle\langle g| - \frac{1}{2} \left\{ |T\rangle\langle T|, \rho \right\} \right). \quad (9)$$

Distinguishing between the desirable target process and the wasteful recombination leads to a time-dependent definition of efficiency as the probability of an excitation moving from $|T\rangle$ to $|g\rangle$ via the target process within a period of time t :

$$\eta(t) = \int_0^t k_T \langle T| \rho(\tau) |T\rangle d\tau. \quad (10)$$

If no time is specified, the efficiency refers to the long-time efficiency $\eta = \lim_{t \rightarrow \infty} \eta(t)$.

Finally, we assume that the effect of the bath on the excited-state dynamics is weak and can therefore be described using Redfield theory to obtain [32, 33]

$$\begin{aligned} \mathcal{R}\rho = & \sum_{ab,cd} \Gamma_{ab,cd}(\omega_{dc}) (M_{cd}\rho M_{ab} - M_{ab}M_{cd}\rho) \\ & + \Gamma_{dc,ba}(\omega_{ab}) (M_{cd}\rho M_{ab} - \rho M_{ab}M_{cd}), \end{aligned} \quad (11)$$

$$\Gamma_{ab,cd}(\omega) = \sum_u \text{Re} \left[\langle a|u\rangle\langle u|b\rangle\langle c|u\rangle\langle u|d\rangle \int_0^\infty C(t)e^{i\omega t} dt \right] \\ = \frac{1}{2} \sum_u \langle a|u\rangle\langle u|b\rangle\langle c|u\rangle\langle u|d\rangle \tilde{C}(\omega), \quad (12)$$

where $M_{ab} = |a\rangle\langle b|$ (with eigenstates $|a\rangle$ and $|b\rangle$ of H_S) and where we ignored the Lamb shift caused by H_{SB} , which could instead be accounted for by redefining H_S [32, 33]. $C(t)$ is the bath correlation function, with the Fourier transform $\tilde{C}(\omega) = 2\pi\omega^2(n(\omega) + 1)(J(\omega) - J(-\omega))$ [32], where $n(\omega)$ is the Bose-Einstein distribution for a bath with temperature $T = 300$ K and $J(\omega) = \sum_\xi g(\omega_\xi)^2 \delta(\omega - \omega_\xi)$ is the bath spectral density. In eq. 12 we have assumed identical spectral densities on all sites, and that the states of the baths at each site are uncorrelated at all times. It can be seen that $\tilde{C}(0) = 0$, which implies that interaction of a system with a bath of harmonic oscillators does not cause any pure dephasing of system eigenstates [32]. We emphasise that \mathcal{R} only models excited state dynamics, and any transfers to $|g\rangle$ are mediated by \mathcal{L}_g and \mathcal{L}_T (see Figure 1c).

It can be shown that each term in eq. 11 leads to time evolution that oscillates at a frequency $\omega_{ab} - \omega_{dc}$, where $\omega_{ab} = (E_a - E_b)/\hbar$. Often, these rates are sufficiently fast for the influence of particular terms to average to zero after sufficient time propagation. This motivates the widely used secular approximation, where all terms for which $|\omega_{ab} - \omega_{cd}| \neq 0$ are discarded [32, 33], eliminating all terms that transfer populations to coherences (and vice versa) and resulting in decoupled population and coherence dynamics. However, if two levels are nearly degenerate, the energy difference between them may be sufficiently small for some terms to oscillate slowly enough to have a significant effect on population dynamics, making it unsafe to discard them [34, 35]. Because the efficiency depends only on populations, the only way for coherences to influence the efficiency is if coherence-to-population transfer can occur; therefore, non-secular effects, found in the limit of nearly degenerate states, are essential for coherent efficiency enhancements.

Here, we treat a system of three sites, the left donor $|L\rangle$, the right donor $|R\rangle$, and the acceptor $|A\rangle$. We assume the two donors have degenerate excited states, so $\epsilon_L = \epsilon_R \equiv \epsilon_D$ and we let $\epsilon_A = \epsilon_D - \Delta$, where Δ is an energy detuning. For $\Delta \gg J_{LR}$, by diagonalising H_S we obtain two eigenstates that are approximately delocalised exclusively across the two donors,

$$|+\rangle \approx \sqrt{p_1}|L\rangle + \sqrt{p_2}|R\rangle \quad (13a)$$

$$|-\rangle \approx \sqrt{p_2}|L\rangle - \sqrt{p_1}|R\rangle \quad (13b)$$

with energies $E_\pm \approx \epsilon_D \pm J_{LR}$ and $p_1 + p_2 = 1$. In general, these two eigenstates also overlap with $|A\rangle$; however, in this regime, this overlap is small enough that we can assume the eigenstates are contained within the donor dimer, and we refer to them as donor eigenstates. In addition, the third energy eigenstate $|A'\rangle$ coincides with $|A\rangle$, up to a small perturbation, and we refer to it as the acceptor eigenstate. All the eigenstates are shown in Figure 1c. Nevertheless, to ensure accurate rates in the Redfield tensor (eq. 11), the calculations below include the small overlaps of the donor eigenstates with $|A\rangle$ and of $|A'\rangle$ with the donor sites.

To demonstrate that the efficiency can be affected by coherences between donor eigenstates, we consider cases where ω_{+-} is smaller than the donor-to-acceptor exciton transfer rate. In this regime, non-secular terms oscillating at frequencies less than $2|\omega_{+-}|$ can have a significant effect on system dynamics. All other non-secular terms—namely those connecting populations to coherences involving the acceptor—oscillate quickly and can be neglected, i.e., we carry out a secular approximation on acceptor states. After this approximation, the \mathcal{R} -induced evolution of each RDO element is

$$(\dot{\rho}_{++})^{\mathcal{R}} = \sum_{a=-,A'} (k_{+a}\rho_{aa} - k_{a+}\rho_{++}) - \alpha \text{Re}[\rho_{+-}], \quad (14a)$$

$$(\dot{\rho}_{--})^{\mathcal{R}} = \sum_{a=+,A'} (k_{-a}\rho_{aa} - k_{a-}\rho_{--}) - \alpha \text{Re}[\rho_{+-}], \quad (14b)$$

$$(\dot{\rho}_{A'A'})^{\mathcal{R}} = \sum_{a=+,-} (k_{A'a}\rho_{aa} - k_{aA'}\rho_{A'A'}) + 2\alpha \text{Re}[\rho_{+-}], \quad (14c)$$

$$(\dot{\rho}_{+-})^{\mathcal{R}} = -\frac{1}{2} \left(\sum_{a=-,A'} k_{a+} + \sum_{b=+,A'} k_{b-} \right) \rho_{+-} \\ + \frac{1}{2} (k_{+-} + k_{-+}) \rho_{-+} \\ + \frac{\alpha}{2} (2e^{-\hbar\omega_{DA'}/k_B T} \rho_{A'A'} - \rho_{++} - \rho_{--}) \\ + \beta (\rho_{++} - e^{-\hbar\omega_{+-}/k_B T} \rho_{--}), \quad (14d)$$

where the population transfer rate from $|a\rangle$ to $|b\rangle$ is $k_{ba} = 2\Gamma_{ab,ba}(\omega_{ab})$, $\omega_{DA'} = (\omega_{+A'} + \omega_{-A'})/2$, $\alpha = 2\Gamma_{+A',A'-}(\omega_{DA'})$ and $\beta = \Gamma_{+-,-+}(\omega_{+-}) - \Gamma_{-,-,+}(\omega_{+-})$. We have also assumed that $\tilde{C}(\omega)$ is slowly varying over the interval $[\omega_{-A'}, \omega_{+A'}]$ and can be replaced with the constant $\tilde{C}(\omega_{DA'})$. The first term in each of these equations contains the secular incoherent rates, while the remaining, non-secular terms account for coherent effects that are non-negligible in the limit of small J_{LR} .

The initial state that is subject to this evolution can be generated by optical excitation. To control the initial state, the individual eigenstates should be individually addressable by different optical modes. In principle, the modes could be different light frequencies, but, in our case, the eigenstates are significantly lifetime broadened by their fast decay, which may make it impossible to resolve them spectrally. This difficulty can be overcome by also considering optical modes with different polarisation.

The initial state depends on whether the exciting light is coherent or incoherent (or, in the case of polarisation, polarised or unpolarised) [15–17]. Weak coherent light prepares the excited state [15, 23, 30, 31, 33]

$$|\psi_{\text{coh}}\rangle = \frac{1}{\sqrt{\mathcal{N}}} \sum_a |\boldsymbol{\mu}_{ag} \cdot \boldsymbol{\mathcal{E}}_a| e^{i\phi_a} |a\rangle, \quad (15)$$

where $\boldsymbol{\mathcal{E}}_a$ and ϕ_a are the electric field amplitude and the phase of the light mode exciting eigenstate $|a\rangle$, $\boldsymbol{\mu}_{ag}$ is the transition dipole moment for the $g \rightarrow a$ transition

and \mathcal{N} is a normalisation factor. The transition dipole moments of the eigenstates are linear combinations of the site-basis transition dipoles, $\boldsymbol{\mu}_{ag} = \sum_u \langle u|a \rangle \boldsymbol{\mu}_{ug}$.

By contrast, incoherent light excites a statistical mixture of eigenstates [15–17]. Because incoherent light is stationary, it, strictly speaking, exists only as a continuous-wave process (various artefacts are present if incoherent light is suddenly switched on [35–40]). However, Jesenko and Žnidarič have shown that the efficiency of light harvesting in continuous-wave incoherent light is equal to the efficiency given a particular transient initial state [41]. In our case, the equivalent initial state is

$$\rho_{\text{inc}} = \frac{1}{\mathcal{N}} \sum_a |\mu_{ag}|^2 \overline{\mathcal{E}_a^2} |a\rangle\langle a|, \quad (16)$$

where μ_{ag} is the magnitude of $\boldsymbol{\mu}_{ag}$ and $\overline{\mathcal{E}_a^2}$ is the ensemble root-mean-square electric field intensity of the mode \mathcal{E}_a .

To maximise coherence magnitudes in the coherent excitations, we consider the case of light sources which excite equal populations in the $|+\rangle$ and $|-\rangle$ states. We also assume that the target process modelled by eq. 9 occurs via the acceptor eigenstate $|A'\rangle$ (i.e., $|T\rangle = |A'\rangle$). Finally, we assume that there is no direct excitation of state $|A'\rangle$, which could trivially contribute to the efficiency. Practically, this would correspond to an excitation by a light source with no electric field component resonant with this state. This ensures that the target process efficiency is an indicator of successful transfers from donor states to the acceptor state. In order to individually address the $|+\rangle$ and $|-\rangle$ states, we choose donor sites with perpendicular dipole moments of equal magnitude. This arrangement results in donor eigenstates whose dipole moments are also perpendicular and of equal magnitude, making them addressable using separate polarisation modes of the light (Figure 1b).

The initial states of the system is then

$$\rho_{\text{inc}} = \frac{1}{2} (|+\rangle\langle +| + |-\rangle\langle -|), \quad (17)$$

for an incoherent (unpolarised) excitation, and

$$\rho_{\text{coh}}(\phi) = |\psi_{\text{coh}}(\phi)\rangle\langle\psi_{\text{coh}}(\phi)|, \quad (18a)$$

$$|\psi_{\text{coh}}(\phi)\rangle = \frac{1}{\sqrt{2}} (|+\rangle + e^{i\phi}|-\rangle), \quad (18b)$$

for a coherent (polarised) excitation with relative phase $\phi = \phi_- - \phi_+$ between the two light modes.

In the limit of eq. 13, exciton populations on sites L and R , given initial state $|\psi_{\text{coh}}(\phi)\rangle$, are

$$\rho_{LL} \approx \frac{1}{2} + \sqrt{p_1 p_2} \cos \phi, \quad (19a)$$

$$\rho_{RR} \approx \frac{1}{2} - \sqrt{p_1 p_2} \cos \phi. \quad (19b)$$

By choosing the phase ϕ , the initial excitations can be significantly localised on the left or the right site, especially for small J_{RA} , when p_1 and p_2 are both close to $\frac{1}{2}$. In particular, population in L is maximised for $\phi = 0$, while that in R is maximised at $\phi = \pi$.

For concreteness, we consider the donors to have energies $\epsilon_D = 2.1$ eV and all three sites to have transition dipole moments of $\mu_{ug} = 7D$, with geometry shown in

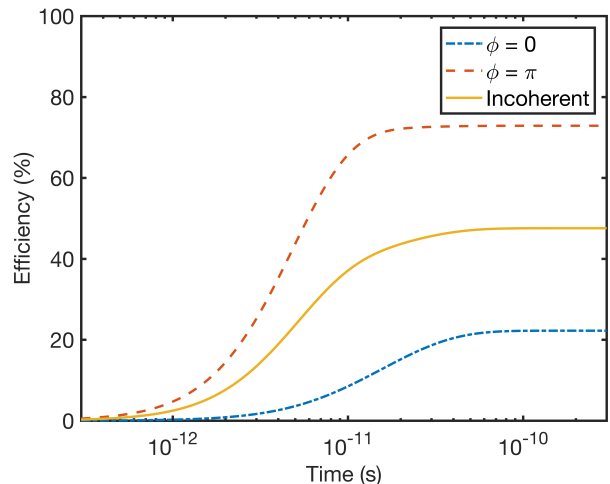


Figure 3. Efficiency under three different excitation conditions. The efficiency is the probability that the exciton reaches the acceptor by a given time, depending on whether initial exciton populations are maximised at R (red), at L (blue) or in an equal mixture of the two (yellow). The overall efficiency at long times can be greatly enhanced by using the optimal initial state.

Figure 1. The separation between the two donors was fixed at $R_{LR} = 2$ nm, corresponding to a donor-donor coupling $J_{LR} = 1.4$ meV and chosen to ensure that $|\omega_{+-}|$ is significantly smaller than the rate of donor-acceptor transfers. The bath was assumed to have a Debye spectral density [32, 42],

$$\omega^2 J(\omega) = \theta(\omega) \frac{2\Lambda\omega_D\omega}{\hbar(\omega^2 + \omega_D^2)}, \quad (20)$$

with reorganisation energy $\Lambda = 140$ cm $^{-1}$ and Debye frequency $\omega_D = 100$ cm $^{-1}$, where $\theta(\omega)$ is the Heaviside step function. We chose a rapid target rate $k_T = 300$ ns $^{-1}$ and a recombination rate $k_g = 50$ ns $^{-1}$.

We used eq. 6, with the full Redfield tensor of eq. 11, to evolve three initial states: the coherent states $\rho_{\text{coh}}(0)$ and $\rho_{\text{coh}}(\pi)$, and the incoherent state ρ_{inc} . We emphasise that the diagonal RDO elements are initially identical across the three cases, and all differences in exciton dynamics and efficiencies are caused by the coherences.

Figure 3 shows that initial coherence can profoundly affect the efficiency by comparing the time-dependent efficiency for the coherent and incoherent excitations, all computed for $\Delta = 60J_{LR}$ and with R_{RA} chosen so that $J_{RA} = 6J_{LR}$. As shown in Figure 2, coherently increasing exciton populations in R significantly increases the efficiency by starting the excitation closer to the acceptor. The observed enhancement is an example of environment-assisted single-photon coherent phase control [43–45]. In this example, the difference in efficiency between the $\phi = \pi$ case and the incoherent case is 25 percentage points. The maximum enhancement is 50 percentage points (a doubling), because the efficiency of the incoherent excitation is always the average of the two coherent efficiencies. This is because the efficiency is a linear function of the initial RDO and $\rho_{\text{inc}} = (\rho_{\text{coh}}(0) + \rho_{\text{coh}}(\pi))/2$.

To explore the limits of coherent efficiency enhancements, we simulated the system for a range of Δ and

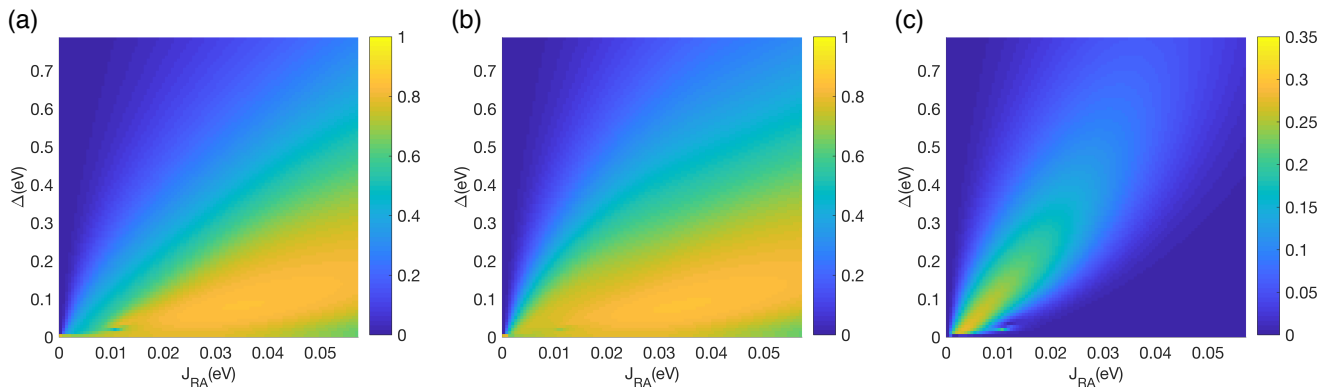


Figure 4. Light-harvesting efficiency for (a) excitations caused by incoherent light, (b) coherent excitations with phase $\phi = \pi$ and (c) the difference between the two, for a range of donor-acceptor detunings Δ and couplings J_{RA} between $|R\rangle$ and the acceptor, evaluated with the full Redfield tensor of eq. 11. The coupling J_{LR} between the two donors is held fixed at $J_{LR} = 1.4$ meV. The coherent enhancement of exciton populations of $|R\rangle$ enhances the efficiency most significantly when neither Δ or J_{RA} is too large.

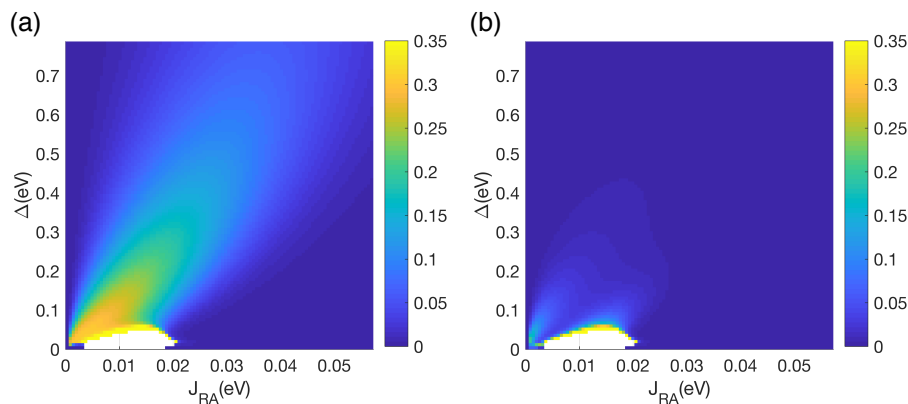


Figure 5. (a) The behaviour in Figure 4 is well reproduced by a simplified Lindblad equation (eq. 14). (b) The difference between the two models (Figures 4c and 5a) is small, except when Δ and J_{RA} are both small, which is when the secular approximation on the acceptor state fails, sometimes causing non-physical behaviour (white region).

R_{RA} , whilst holding R_{LR} fixed. Figure 4 compares incoherent efficiencies (Figure 4a) with those of coherent excitations with phase $\phi = \pi$ (Figure 4b). For simplicity, the results are shown as functions of J_{RA} instead of R_{RA} ; in all cases, J_{LA} is much less than J_{RA} and has a minor effect on the efficiency. Figure 4c shows that there is a distinct region where the coherent efficiency can exceed the incoherent one by as much as 30 percentage points. By contrast, when Δ is small and J_{RA} large, Figures 4a and 4b show that donor-to-acceptor transfer is fast enough for efficiencies to be large for both excitation conditions, preventing a large enhancement. On the other hand, when Δ is large and J_{RA} small, donor-to-acceptor coupling is too small for transfer rates to compete with the recombination rate, giving a low efficiency regardless of initial state.

Similar results can be obtained by propagating the approximate master equation in eq. 14, as shown in Figure 5. Across most of the parameter space, there is little difference between the estimated efficiency enhancements obtained from the full Redfield tensor and the approximate model, validating the simpler eq. 14 as a way to understand the origin and limitations of coherent efficiency enhancements.

The cause of efficiency enhancement are population transfers from the donor states to the acceptor that are

mediated by the non-secular terms (those proportional to α) in eqs. 14a, 14b and 14c. In our case $\alpha < 0$, so a negative $\text{Re}[\rho_{+-}]$ causes a decrease in donor populations and an increase in acceptor populations, while a positive $\text{Re}[\rho_{+-}]$ has the opposite effect. Since $\text{Re}[\rho_{+-}]$ is negative when $\phi = \pi$, observed donor-acceptor transfer rates are fastest when populations at R are maximised. Furthermore, the sum of the additional terms is always 0, ensuring that eq. 14 is trace preserving.

In addition, because $\rho_{+-} - \rho_{-+} = 2i \text{Im}[\rho_{+-}]$, the dephasing terms proportional to k_{+-} in eq. (14d) matter only when ρ_{+-} has an imaginary component. Since our initial states have real coherences, in the limit $\omega_{+-} \ll (k_{A'+} + k_{A'-})/2$, the coherence ρ_{+-} oscillates too slowly for its imaginary component to gain significant magnitude before the excitation transfers to the acceptor. Therefore, and due to the absence of pure dephasing, the coherences survive and maintain a positive real part long enough for the enhancements proportional to α to be significant.

The approximate eq. 14 fails in the lower left part of Figure 5. This region is where the secular approximation with respect to the acceptor site fails. We assumed in eq. 14 that terms oscillating at frequency $|\omega_{\pm A'}|$ can be discarded due to their rapid oscillation, but this assumption fails when Δ is small. In some cases, indicated with

the white region in Figure 5, an efficiency could not be computed because the failure of the approximation led to populations becoming unphysical (either negative or greater than 1).

In summary, we have shown that excitonic coherences can significantly affect energy-transfer efficiency in a light-harvesting system. The coherences can be controlled by controlling the coherence of the exciting light; compared to incoherent excitation, engineered coherent light can double the light-harvesting efficiency for a dimeric donor. In larger systems, the enhancement could be even larger. The particular parameter regimes we explored were chosen to be realisable in engineered nanostructures, providing a platform for the development of

new, quantum-inspired light-harvesting technologies.

Acknowledgements: We thank Andrew Doherty, Jacob Krich, Albert Stolow, and Joel Yuen-Zhou for valuable discussions. S.T. and I.K. were supported by the Westpac Bicentennial Foundation through a Westpac Research Fellowship, by the Australian Research Council through a Discovery Early Career Researcher Award (DE140100433), by an Australian Government Research Training Program (RTP) Scholarship, and by a scholarship from the University of Sydney Nano Institute. S.B. was supported in part by the U.S. National Science Foundation, Grant No. PHYS-1630114. S.R.-K. acknowledges financial support from the German Academic Exchange Service (DAAD) and Iran's National Elites Foundation (INEF).

-
- * Email: ivan.kassal@sydney.edu.au
- [1] G. S. Engel, T. R. Calhoun, E. L. Read, T. K. Ahn, T. Mancal, Y. C. Cheng, R. E. Blankenship, and G. R. Fleming, *Nature* **446**, 782 (2007).
 - [2] G. Panitchayangkoon, D. Hayes, K. A. Fransted, J. R. Caram, E. Harel, J. Wen, R. E. Blankenship, and G. S. Engel, *Proc. Natl. Acad. Sci.* **107**, 12766 (2010).
 - [3] E. Collini, C. Y. Wong, K. E. Wilk, P. M. G. Curmi, P. Brumer, and G. D. Scholes, *Nature* **463**, 644 (2010).
 - [4] H. Lee, Y. C. Cheng, and G. R. Fleming, *Science* **316**, 1462 (2007).
 - [5] D. Hayes, G. B. Griffin, and G. S. Engel, *Science* **340**, 1431 (2013).
 - [6] G. D. Scholes, *Phys. Chem. Lett.* **1**, 2 (2010).
 - [7] G. D. Scholes, G. R. Fleming, A. Olaya-castro, and R. V. Grondelle, *Nature* **3**, 763 (2011).
 - [8] I. Kassal, J. Yuen-Zhou, and S. Rahimi-Keshari, *Phys. Chem. Lett.* **4**, 362 (2013).
 - [9] F. Fassioli, R. Dinshaw, P. C. Arpin, and G. D. Scholes, *Royal Soc. Int.* **11**, 20130901 (2013).
 - [10] G. D. Scholes, G. R. Fleming, L. X. Chen, A. Aspuru-guzik, A. Buchleitner, D. F. Coker, G. S. Engel, R. V. Grondelle, A. Ishizaki, D. M. Jonas, J. S. Lundeen, J. K. McCusker, S. Mukamel, J. P. Ogilvie, A. Olaya-Castro, M. A. Ratner, F. C. Spano, K. B. Whaley, and X. Zhu, *Nature* **543**, 647 (2017).
 - [11] E. Romero, V. I. Novoderezhkin, and R. van Grondelle, *Nature* **543**, 355 (2017).
 - [12] N. Christensson, *J. Phys. Chem. B* **116**, 7449 (2012).
 - [13] V. Tiwari, W. K. Peters, and D. M. Jonas, *Proc. Natl. Acad. Sci.* **110**, 1203 (2013).
 - [14] E. Thyryhaug, R. Tempelaar, M. J. Alcocer, K. Zidek, D. Bina, J. Knoester, T. L. Jansen, and D. Zigmantas, *Nature Chem.* **10**, 780 (2018).
 - [15] X. P. Jiang and P. Brumer, *J. Chem. Phys.* **94**, 5833 (1991).
 - [16] T. Mančal and L. Valkunas, *New Journal of Physics* **12**, 065044 (2010).
 - [17] P. Brumer and M. Shapiro, *Proc. Natl. Acad. Sci.* **109**, 19575 (2012).
 - [18] K. E. Dorfman, D. V. Voronine, S. Mukamel, and M. O. Scully, *Proc. Natl. Acad. Sci.* **110**, 2746 (2013).
 - [19] A. A. Svidzinsky, K. E. Dorfman, and M. O. Scully, *Phys. Rev. A* **84**, 1 (2011).
 - [20] M. O. Scully, *Phys. Rev. Lett.* **104**, 1 (2010).
 - [21] M. O. Scully, K. R. Chapin, K. E. Dorfman, M. B. Kim, and A. Svidzinsky, *Proc. Natl. Acad. Sci.* **108**, 15097 (2011).
 - [22] C. Creatore, M. A. Parker, S. Emmott, and A. W. Chin, *Phys. Rev. Lett.* **111**, 1 (2013).
 - [23] R. D. J. León-Montiel, I. Kassal, and J. P. Torres, *J. Phys. Chem. B* **118**, 10588 (2014).
 - [24] S. Baghbanzadeh and I. Kassal, *Phys. Chem. Lett.* **7**, 3804 (2016).
 - [25] S. Baghbanzadeh and I. Kassal, *J. Phys. Chem. Chem. Phys.* **18**, 7459 (2016).
 - [26] J. Herek, W. Wohlleben, R. Cogdell, D. Zeidler, and M. Motzkus, *Nature* **417**, 533 (2002).
 - [27] J. Savolainen, R. Fanciulli, N. Dijkhuizen, A. L. Moore, J. Hauer, T. Backup, M. Motzkus, and J. L. Herek, *Proc. Natl. Acad. Sci.* **105**, 7641 (2008).
 - [28] S. Hoyer, F. Caruso, S. Montangero, M. Sarovar, T. Calarco, M. B. Plenio, and K. B. Whaley, *New J. Phys.* **16**, 045007 (2014).
 - [29] F. Caruso, S. Montangero, T. Calarco, S. F. Huelga, and M. B. Plenio, *Phys. Rev. A* **85**, 042331 (2012).
 - [30] M. Shapiro and P. Brumer, *Quantum Control of Molecular Processes*, 2nd ed. (Wiley, 2012).
 - [31] B. Brüggemann and V. May, *J. Phys. Chem. B* **108**, 10529 (2004).
 - [32] V. May and O. Kühn, *Charge and Energy Transfer Dynamics in Molecular Systems*, 3rd ed. (Wiley, 2011).
 - [33] H. P. Breuer and F. Petruccione, *The Theory of Open Quantum Systems*, 1st ed. (Oxford, 2006).
 - [34] A. Dodin, T. Tscherbul, R. Alicki, A. Vutha, and P. Brumer, *Phys. Rev. A* **97**, 013421 (2018).
 - [35] T. V. Tscherbul and P. Brumer, *Phys. Rev. Lett.* **113**, 1 (2014).
 - [36] T. V. Tscherbul and P. Brumer, *J. Chem. Phys.* **142**, 104107 (2015).
 - [37] T. Grinev and P. Brumer, *J. Chem. Phys.* **143**, 244313 (2015).
 - [38] A. Dodin, T. V. Tscherbul, and P. Brumer, *J. Chem. Phys.* **144**, 244108 (2016).
 - [39] A. Dodin, T. V. Tscherbul, and P. Brumer, *J. Chem. Phys.* **145**, 244313 (2016).
 - [40] J. Olšina, A. G. Dijkstra, C. Wang, and J. Cao, *arXiv* **1408**, 5385 (2014).
 - [41] S. Jesenko and M. Žnidarič, *J. Chem. Phys.* **138**, 174103 (2013).
 - [42] L. A. Pachon, J. D. Botero, and P. Brumer, *J. Phys. B* **50**, 184003 (2017).
 - [43] P. Brumer and M. Shapiro, *Chem. Phys.* **139**, 221 (1989).
 - [44] M. Spanner, C. A. Arango, and P. Brumer, *J. Chem. Phys.* **133**, 151101 (2010).
 - [45] C. A. Arango and P. Brumer, *J. Chem. Phys.* **138**, 071104 (2013).